NAIC-ID(RS)T-0407-94

NATIONAL AIR INTELLIGENCE CENTER

APPLICATIONS OF ORGANIC AND POLYMER NONLINEAR OPTICAL MATERIALS IN OPTICS COMPUTATIONS

by

Sun Maocong, Ji Suling, Li Chunfei

HUMAN TRANSLATION

NAIC-ID(RS)T-0407-94 27 March 1995

MICROFICHE NR: 95C000114

APPLICATIONS OF ORGANIC AND POLYMER NONLINEAR OPTICAL MATERIALS IN OPTICS COMPUTATIONS

By: Sun Maocong, Ji Suling, Li Chunfei

English pages: 17

Source: Wuli, Vol. 20, Nr. 6, June 1991; pp. 361-365

Country of origin: China
Translated by: Leo Kanner Associates
F33657-88-D-2188
Requester: NAIC/TATA/J.M. Finley
Approved for public release; Distribution unlimited.

GRAPHICS DISCLAIMER

All figures, graphics, tables, equations, etc. merged into this translation were extracted from the best quality copy available.

APPLICATIONS OF ORGANIC AND POLYMER NONLINEAR OPTICAL MATERIALS IN OPTICS COMPUTATIONS

Sun Maocong, Ji Suling, and Li Chunfei; Sun and Ji of department of optics, Shandong University, Jinan, 250100; and Li of department of applied physics, Harbin Industrial University, Harbin, 150006

[Abstract] Organic and polymer nonlinear optical materials have good properties in optics, structure, and mechanics. At present, such materials are undergoing rapid development. This article emphasizes presenting some typical organic and polymer nonlinear optical materials, describes the optical bistability devices, optical power restraining units, spatial optical modulators, and optical waveguides fabricated from these materials. By comparing the organic crystals and semiconductor devices of the same categories, the article reports on the potential priorities and application prospects in the field of optics computations by using these organic and polymer nonlinear materials.

In nonlinear optics, organic and polymer materials are emphasized by researchers [1]. These kinds of materials exhibit

many excellent properties [2]. In optics, these materials have high light-loss thresholds, as well as wide wavebands for light passage; the range of response time is between seconds to femtoseconds. In appearance, these materials can be block crystals, liquid or solid solutions, as well as thin films and multilayer films of various thicknesses. As to their properties in mechanics, these materials resist radiation and impact with high mechanical strength. These excellent properties make possible the applications of organic and polymer materials in the development of all-optical computers with superhigh speeds and large capacity.

I. Optical Bistability Devices

Optical bistability devices are important components in realizing optical switching and optical computations. Used in fabricating optical bistability devices, these optical materials include mainly organics (dyestuffs and liquid crystals) and a series of semiconductor materials, which generally have relatively high third-order nonlinear effects. However, some organic and polymer materials such as polydiethine (PDA), similarly exhibit high third-order nonlinear effects. As indicated in a theoretical analysis [3], the pure electron third-order nonlinear polarization $khi^{(3)}$ of organic materials can be $1x10^{-8}$ e.s.u., and its response time can be as short as femto-seconds.

PTS stands for a diethine derivative with side radicals as p-toluene sulfonate. Soaking the PTS polymer crystals in

methylene iodide with matching refractive index and then placing the crystals between two mirrors with a 95% reflective index, in this way, a nonlinear Fabry-Perot (F-P)* device is formed. By using excited Raman scattered light (with a wavelength of 1.9micrometers) generated in hydrogen gas with an Nd:YAG laser as the light source, the polarization direction of the light is parallel to the axial direction of the main chain of the crystal. At different laser intensities, on relations between pulse energy and the device's optical thickness measured with a measuring apparatus, thus the function curves were plotted. As shown in Fig. 1, when the laser intensity exceeds $3MW/cm^2$, the peak value locations of the curve begin to move, and the height of the peak value begins declining, thus exhibiting the property of nonlinearity with respect to transmission. As indicated in experimental measurements, the $khi^{(3)}$ of the PTS polymer crystals is $5x10^{-10}$ e.s.u. in the transparent zone; at the absorption edge of 651.5nm, it is $9x10^{-9}$ e.s.u.[4]; its nonlinear refractive index n_2 is $1.8x10^{-6}$ $(MW/cm^2)^{-1}$ [5]. In the above-mentioned F-P device, its nonlinearity effect is due to the high third-order optical nonlinearity of the PTS polymer crystals.

Heat-caused changes in the refractive index represent one of the regimes generated by optical bistability. When semiconductor materials (such as zinc selenide) employed in these experiments, generally the experiments should be conducted in the vicinity of

* J.P. Hermann et al., Digest of Tech. Papers from XI Int. Quantum; Electron. Conf. (1980), 656.

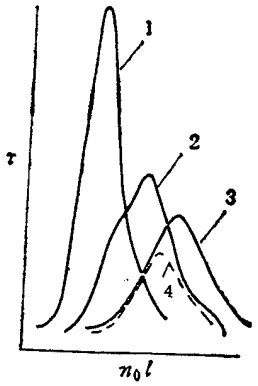

Fig. 1. Relationship curves between pulse energy and optical thickness $n_0 l$ after passing through Fabry-Perot interferometer
LEGEND: Laser intensities (peak intensities at focal points) corresponding to the four curves are as follows:

1. <3MW/cm²; 2. 18MW/cm²; 3. 45MW/cm²; 4. 70MW/cm²

the band gap [6]. The problem of matching these materials and the laser light source is relatively marked. It is relatively convenient to use polymer diethine material in these experiments. Polymer diethine has intensive absorption spectral lines with widths exceeding 100nm. With different environments and polymer side chains, the corresponding absorption maximum values exist, respectively, at 470, 530, and 620nm. By blending with antimony or iodine pentachloride, further absorption can be produced in the near infrared zone exceeding 1micrometer wavelength. A soluble polydiethine material [7] has been applied in the experiments of heat-caused optical bistability [8]. There are two types of specimens used in the experiments: the first type is a solution of polydiethine and toluene, and the second type is thin films of a mixture of polydiethine and polyethylenechloride.

By changing the concentrations of polydiethine in the specimen, the optical absorption properties of the specimen can be adjusted. If the specimen thickness L=1mm, the laser wavelength is 514nm. When changing the concentration of polydiethine so that the transmissibility T is 0.57, the corresponding absorption coefficient alpha=-ln(T)/L = $562nm^{-1}$. For the first type of specimens, with measurement two bistability curves are obtained: a bistability curve of transmission and incident laser power, and another bistability curve of phase conjugate reflective index, and incident pumping light intensity. As shown by the curves, the switching power is 3.9mW. For the second specimen, through experiments optical bistability is similarly observed. The heat-caused nonlinearity of the polydiethine material is due to nonradiative relaxation of the excited state of polydiethine (especially in solution). In degenerative four-wave mixing frequency, this heat-caused nonlinearity brings about local change in temperature with refractive index; thus, a phase grating is formed in the mixing-frequency medium. In some inorganic semiconductors (such as indium antimonide) and multi-quantum well structures, third-order nonlinear polarization with numerical magnitude of 1e.s.u. has been obtained. As indicated by experimental and theoretical analysis on heat-caused optical bistability of polydiethine, similar or even higher third-order nonlinear polarization can be obtained for heat-caused nonlinearity of organic materials.

In Section IV of this article, the authors will introduce an

optical bistability device consisting of Langmuir-Bloquet (LB) thin-film waveguide of polydiethine.

A highly concentrated fluorescein dye solution and a 2micrometer-thick fluorescein plexiglass (PMMA) thin film can also be used to generate an optical bistability delay response [9]. In the highly concentrated fluorescein dye solution, most dyes exist in dimeric form. When excited with a high-intensity laser, the dimers are cracked into monomers, so that the absorption coefficient is related to laser intensity. Therefore, highly concentrated fluorescein dye solution is a nonlinear absorption medium; in this medium, optical bistability should be observed [10,11].

II. Restrictions on Optical Power

The main obstacles to obtaining useful optical power limiters are the high threshold switching value and the low light-loss thresholds. To overcome this barrier, researcher attention has been directed to organic and polymer materials with high linearities.

Category III third-order nonlinear organic compounds and polymers were applied for limiting the displayed optical power [12]. The first category is beta-carotene (betaC); its third-order nonlinearity polarity $khi^{(3)}$ is approximately 10^{-11}e.s.u. The cause of the nonlinearity is the electron motion in the nondefinite zone of the pi-electron system of 11 conjugate double chains. The second category is the phenazene compounds. biphenyl phenazine dimer (BBP) is one of this category of

compounds. In this category of materials, the regime of nonlinear response is related to the electric charge transfer of radical cations. The third category is the aromatic hetero-cyclic polymers; poly-alpha-5,5'-dithiophenebenzal radical (PBTB) is one of the chemicals. By using a nanosecond Q-switch Nd:YAG laser to illuminate a 1cm-thick liquid specimen or a 10micrometer-thick solid thin film in measuring the properties after the light has passed through the specimen, the nonlinear absorption coefficient $alpha_2$ and the nonlinear refractive index n_2 of the three materials are obtained, as shown in Table 1. Fig. 2 shows the optical power limiting function observed for PBTB. As obtained in the experiments, the intensity limiting threshold value is as low as 10MW/cm^2; however, the laser-loss threshold is higher than 10GW/cm^2. Nonlinear polymers are very promising to be used to limit optical power.

TABLE 1. Properties of Three Categories of Nonlinear Optical Materials

材料 (1)	标定浓度 (克分子浓度) (2)	非线性阈值 (W/cm^2) (3)	α_2 (cm/W)	n_2 (cm^2/W)
βC	9.4×10^{-3}	3×10^{8}	4.0×10^{-9}	1.4×10^{-12}
BBP	10^{-2}	2×10^{8}	1.6×10^{-8}	4.0×10^{-13}
PBTB	2.0×10^{-3}	10^{7}	3.2×10^{-7}	1.5×10^{-11}

KEY: 1 - Material 2 - Marked concentrations (in g-moles) 3 - Nonlinear threshold value

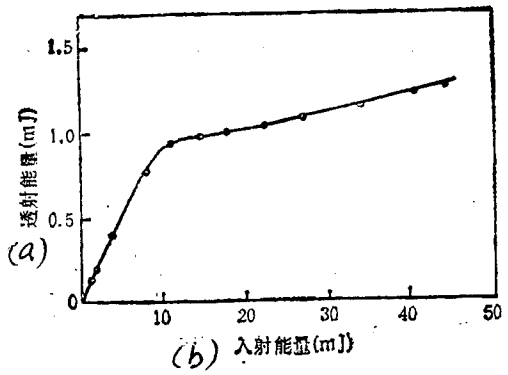

Fig. 2. Optical power limiting function of PBTB.
KEY: a - Transmission energy b - Incident energy

III. Space Optical Modulators

Whether the first-order or second-order space optical modulators, previously these optical modulators relied basically on inorganic electrooptical crystals, such as lithium niobate ($LiNBO_3$), bismuth silicate ($Bi_{12}SiO_{20}$), and potassium dideuteriumphosphate (KD^*P). These crystals are high in quality and have complete data available, therefore it is more convenient to use them. As discovered in recent research, the space optical modulators made of organic and polymer materials have unique advantages.

The totally incident reflection space light modulator (TIR SLM) is an attractive first-order electrooptical modulator [13]. Fig. 3 shows the TIR SLM made from the organic crystal 2-methyl-4-nitraniline (NMA). This layout includes a super-large-scale integrated circuit from series to parallel addressing; in this circuit, thousands of transistors provide data. The transistors

are connected with thousands of parallel metal wires on the chip surface. The chips are tightly pressed on the NMA crystal in order to have the margin field among the metal wires to be coupled to the crystals. By means of Pockels' effect, these margin fields change the refractive index of the crystals. When this setup is used to illuminate the horizontal axial collimation sheet-shaped light beams, the light has total incident reflection at the boundary surface. With the light approaching and leaving the boundary surface, the phase shift (related to the refractive index caused by the boundary electric field) is obtained, therefore a change of the electric field modulates the optical phase.

An MNA crystal has high value in generating second-order harmonic waves and linear electrooptical properties. The crystal's electrooptical coefficient nu_{11} is approximately 67 $25x10^{-11}$m/V, at lambda=632.8nm, the refractive index n_x=2.356; n_y=1.774, and n_z=1.452. The low-frequency piezoelectric constants are as follows: ε_x=5.02 and ε_y=3.89.

By comparing the respective uses of the MNA and the $LiNbO_3$ as the TIR SLM for crystal modulation, two ratios R of the TIR SLM phase shifts are introduced. For orthogonal driving

$$R = \frac{n_x^3 \nu_{11}}{n_c^3 \nu_{33}}, \qquad (1)$$

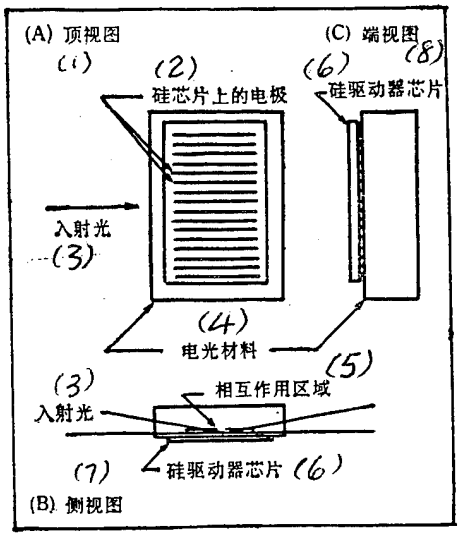

Fig. 3. Three views of total incident reflection space optical modulator
KEY: 1 - Top view 2 - Electrode on silicon chip
3 - Incident light 4 - Electrooptical material
5 - Zone of interaction 6 - Silicon driver chip
7 - Side view 8 - Front view

For tangential driving

$$R = \frac{n_x^3 \nu_{11} \frac{\varepsilon_y}{\varepsilon_x}}{n_c^3 \nu_{33} \frac{\varepsilon_1}{\varepsilon_2}}. \qquad (2)$$

In the two above-mentioned equations, the numerators take on the value of MNA, however, the denominator takes on the value of LINbO3. The relevant data are substituted in Eqs. (1) and (2); the respective values of R are calculated as 2.66 and 1.89. This result explains that, in order to generate the same optical phase modulation, the driving voltage required for the TIR SLM of MNA is reduced to 1/2.5 of the TIR SLM of $LiNbO_3$. For the driving voltage of small phase shift and sine type, the optical

diffraction efficiency is one-half of the phase shift squared. Therefore, under the driving voltage of similar properties, the diffraction efficiency of TIR SLM of MNA is five times greater than of $LiNbO_3$.

Fig. 4 shows an electrooptical space light modulator of reflection; the modulator is composed of an optical receptor, a medium mirror, and electrooptical materials. Generally, an optical receptor is a silicon device with very fast response time (measured in nanoseconds) and high resistivity. The entire modulator is determined by the three following factors with respect to response time of single-frame images: the first factor is the cumulative time of the input light. Within this period of time, the input light can generate sufficient electric charges, and the required modulation obtained with the electrooptical materials. The second factor is the RC time constant of the modulator. The third factor is the intrinsic response time of the electrooptical materials. In the case that the electrooptical material is a KD*P crystal, since the crystal's response time is measured in the subnanoseconds, the frame image cycle of the modulator is determined only by the intensity of the write-in light, and by the modulator's electrical capacity. When KD*P crystal operates in the vicinity of its Curie temperature (-57°C), its electrooptical coefficient is increased. Thus, the bias can be maintained between the breakdown voltage of the optical receptor. However, in the vicinity of the Curie temperature, the piezoelectric constant of the KD*P also

significantly increases. This is not beneficial to modulator efficiency. Since the variation of the polarized optical system with temperature is small, it still requires the same amount of optically generated electric charge to generate a certain phase shift; the cumulative time is not reduced. A large piezoelectric constant of inorganic ferroelectro-optical material is an unavoidable feature. A large electrical capacity, on the contrary, affects the speed and sensitivity for optical addressing that a space light modulator should have. The discriminability of the modulator is also limited to 10 lp/mm.

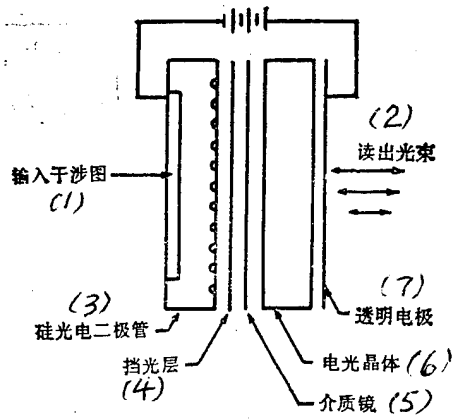

Fig. 4. Schematic diagram of electrooptical space light modulator
KEY: 1 - Input interferogram 2 - Readout light beam 3 - Silicon optoelectronic diode 4 - Light shading layer 5 - Medium mirror 6 - Electrooptical crystal 7 - Transparent electrode

By comparing with inorganic electrooptical crystals, we see that organic thin films not only have large electrooptical coefficients, but also have low piezoelectric constants. This

property of organic thin films can bring about a major improvement on the properties of electroooptical modulators [2]. These space optical modulators of polarized organic thin films (with electrooptical coefficients not much different from that of KD*P crystals, and piezoelectric constant equal to 4) can have the sensitivity of array liquid crystal devices, the speed of KD*P crystal devices, and much better discriminability than either of both these devices. All these new properties are generated by lower thin film electric capacity at room temperature.

In electrooptical devices, the main disadvantages of using organic materials are the limitations on repeatability and optical load because of poor heat conductivity of polymers. Only by properly solving the heat dissipation problem and also considering that organic materials have high light-loss thresholds, can we expect that maximum limit of optical load for the organic electrooptical devices still be much greater than that of inorganic devices.

IV. Integrated Optical Devices

As an example of an organic integrated optical device, two types of organic wave search structures [2] are described in the following. One type is based on the Kerr effect modulators of amorphous MNA thin film; another type is an electrooptical modulator based on PC6S polarized polymer thin films. Both modulators are plate-shaped modulators with structure as shown in Fig. 5. In Fig. 5, the MNA/PMMA guest-host thin film (or PC6S

polymer thin film) is used as the waveguide layer of the modulator; a silica thin film and polysilicaparaffin thin films are two transitional layers in the modulator. From measurements, the half-wave voltage of the electrooptical modulator is about 23V; the frequency response can be approximately 10kHz.

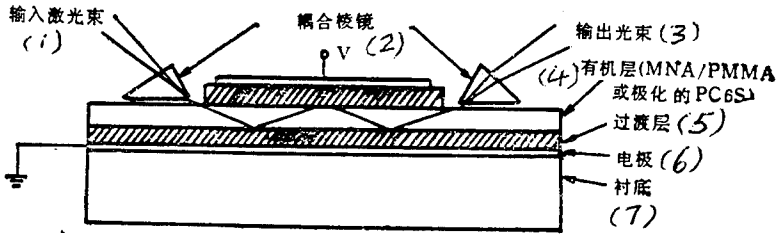

Fig. 5. Schematic diagram of Kerr effect waveguide modulator
KEY: 1 - Input laser beam 2 - Coupled lens 3 - Output light beam 4 - Organic layer (MNA/PMMA or polarized PC6S) 5 - Transitional layer 6 - Electrode 7 - Substrate

There are several methods of fabricating polymer nonlinear waveguides [14]; three of these methods are emphasized and applied. The first method is the solvent pour casting method. For example, 35g of low-molecular-weight PMMA is dissolved in 100mL of ethylacetate-2-ethylene, then 7g of MNA is added. Then the resulting solution is spun and coated onto a substrate of BK7 glass; the rotating speed of 5000rpm and the rotation is continued for 45s. Finally, the specimen is baked at 50°C to remove the solvent. The second method is the solvent-assisted inward diffusion method. In this method, the polymer is soaked

into a hot impurity-doped solution so that the organic impurity-doped molecules diffuse inward onto the surface of the polymer. The main advantage of this method is that the channel waveguide can be determined by using a simple metal pattern printing technique. An aluminum layer is deposited onto the polymer surface; a conventional metal platen printing technique is employed to cause a graph to appear on the aluminum layer. The aluminum-layer graph acts as a film-covering plate so that the dopant impurities can diffuse only by passing through the uncovered regions. By applying this type of method, multipolymer nonpolarized optical waveguides, channel waveguides, and oriented couplers have been fabricated. The third method is the thin-film deposition method, which employs the LB technique. In this method, the penetration can be closely controlled by means of layer thickness and molecular orientation. Without the polarization steps, the arrangement of chromophores can be obtained.

Deposit the polydiethine LB thin films onto a Corning 7059 glass waveguide with high-frequency sputtering, thus obtaining a PDA-LB thin film waveguide. This is a type of a mixer plate-shaped waveguide. Its structural cross-section is shown in Fig. 6. In the PDA-LB mixer thin-film mixer waveguide, two types of total-light bistability are observed [15]. One type of bistability originates in the nonlinear coupling between the lens and the PDA-LB-Corning mixer waveguide. Another type of bistability involves a nonlinear coupling between the wave search

and the distributed Bragg reflector grating in the PDA-LB mixer. Fig. 6(b) shows this waveguide with a distributed Bragg feedback structure. The grating structure is formed by dual light-beam interference of a double-frequency pulse YAG laser (0.543micrometers, approximately 300kW, pulse duration 20ns). As indicated in the experimental results, this distributed Bragg structure has a much lower switching threshold.

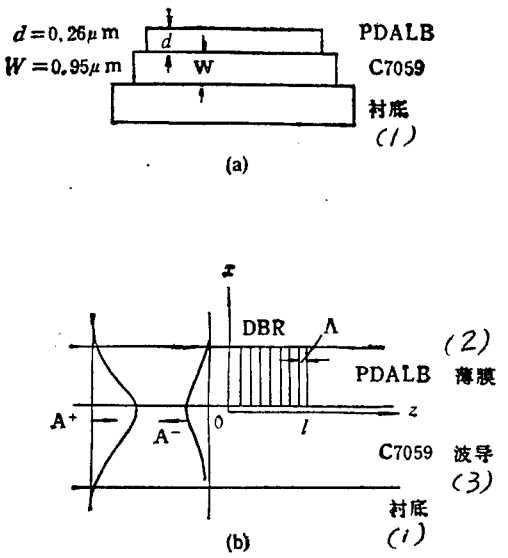

Fig. 6. (a) Fundamental structure of mixer waveguide (b) Fundamental structure of mixer waveguide with distributed Bragg reflector (DBR) structure; LAMBDA is the gap (1.5-1.6micrometer) of grating structure; l is length (3mm) of grating structure
KEY: 1 - Substrate 2 - Thin film 3 - Waveguide

We can clearly see from the above-mentioned descriptions that satisfactory applications have been realized in the various above-mentioned optical devices by using the organic and polymer nonlinear optical materials as a new type of materials. We can

expect that the organic and nonlinear optical materials will have an ever-growing influence in the field of optics computations as research continues to advance.

REFERENCES

[1] Xiao Dingquan and Zheng Wenchen, Wuli [Physics] 14(1985), 463.

[2] R. Lytel et al., *SPIE*, 824(1987), 152.
[3] G. R. Meredith, *Proc. SPIE*, 567(1986), 61.
[4] R. J. Seymour et al., *Proc. SPIE*, 567(1986), 56.
[5] C. Sauteret et al., *Phys. Rev. Lett.*, 36(1976), 956.
[6] S. D. Smith et al., *Optics Commun.*, 51(1984). 357.
[7] C. Plachetta et al., *Makromol. Chem. Rapid Commun.*, 3(1982), 244.
[8] W. Blau, *Optics Commun.*, 64(1987), 85.
[9] Shammai Speiser et al., *SPIE*, 824(1987), 144.
[10] M. Orenstein et al., *Phys. Rev. A*, 35(1987), 1192.
[11] M. Orenstein et al., *Phys. Rev. A*, 35(1987), 2175.
[12] Saukwan Lo et al., *SPIE*, 824(1987), 162.
[13] R. V. Johnson et al., *Optical Eng.*, 22(1983), 665.
[14] J. Brettle et al., *SPIE*, 824(1987), 171.
[15] K. Sasaki et al., *J. Opt. Soc. Am. B*, 5(1988), 457.

DISTRIBUTION LIST

DISTRIBUTION DIRECT TO RECIPIENT

ORGANIZATION	MICROFICHE
B085 DIA/RTS-2FI	1
C509 BALLOC509 BALLISTIC RES LAB	1
C510 R&T LABS/AVEADCOM	1
C513 ARRADCOM	1
C535 AVRADCOM/TSARCOM	1
C539 TRASANA	1
Q592 FSTC	4
Q619 MSIC REDSTONE	1
Q008 NTIC	1
Q043 AFMIC-IS	1
E051 HQ USAF/INET	1
E404 AEDC/DOF	1
E408 AFWL	1
E410 AFDTC/IN	1
E429 SD/IND	1
P005 DOE/ISA/DDI	1
P050 CIA/OCR/ADD/SD	2
1051 AFIT/LDE	1
PO90 NSA/CDB	1
2206 FSL	1

Microfiche Nbr: FTD95C000114
NAIC-ID(RS)T-0407-94